www.ietdl.org

Published in IET Networks
Received on 22nd November 2011
Revised on 27th May 2012
doi: 10.1049/iet-net.2011.0017

ISSN 2047-4954

Performance analysis and optimisation of a cooperative frequency-modulated differential chaos shift keying ultra-wideband system under indoor environments

Y. Fang P. Chen L. Wang

College of Information Science and Technology, Xiamen University, Fujian 361005, People's Republic of China
E-mail: wanglin@xmu.edu.cn

Abstract: A cooperative frequency-modulated differential chaos shift keying (FM-DCSK) ultra-wideband (UWB) systems, named cooperative FM-DCSK UWB system, is investigated under indoor environments of IEEE 802.15.4a in this article. The performance of the cooperative FM-DCSK UWB system is evaluated in such channel models (CMs), that is, CM1–CM4, by means of the moment generating function. Monte Carlo simulation results show that the bit-error-rate performance of the proposed system is much better than the conventional multi-access FM-DCSK UWB system, which is showed to be highly consistent with the theoretical results. The integration interval of the proposed cooperative UWB system is optimised to further improve the system performance through the binary search algorithm. Meanwhile, aiming to provide a good compromise between the system performance and implementation complexity, the number of received antenna at the destination (single-input multiple-output architecture) is also investigated and discussed. For the aforementioned advantages, the proposed system can be seen as a viable alternative to other multi-access FM-DCSK UWB schemes for the low-rate and low-power wireless personal area network and wireless sensor network applications.

1 Introduction

Ultra-wideband (UWB) technology has dramatically received attention as a promising candidate for many indoor communication applications such as wireless personal area networks (WPANs) and wireless sensor networks (WSNs) [1]. A UWB signal has a wide bandwidth, which can be extended from 3.1 to 10.6 GHz, that is, 7.5 GHz, with a low-power spectrum density and therefore makes this technology especially attractive. Several new standards about the UWB technology are under development since their ability to provide WPAN with low-power, low-cost and low-complexity devices. Aiming for low-rate WPAN applications, the IEEE 802.15.4a standard was established in 2007 [2].

Owing to the wideband and no-periodic characters, some chaotic modulation schemes have been proposed as candidates of the UWB standards for WPAN by the IEEE 802.15.4a task group in recent years [3, 4]. Among all the chaotic modulation schemes, frequency-modulated differential chaos shift keying (FM-DCSK) has been proved to have the prominent noise performance and excellent anti-multipath fading capability [5–7]. Consequently, some researchers have focused on using FM-DCSK for UWB transmission [8, 9] and optimising its performance. For instance, some important system parameters have been discussed and optimised in [10], which demonstrated its promising advantages for indoor applications. Besides that, a data-aided timing synchronisation algorithm has also been proposed for the FM-DCSK UWB system to resolve technical difficulties regarding the receiver implementation [11]. However, the performance of the FM-DCSK UWB systems is still limited because of the non-coherent detection and the power loss of the reference pulse.

Recently, cross-layer design [12] and cooperative communication [13–15] have been widely investigated as potential technologies for future wireless networks to further improve their performance. In particular, some cooperative-chaotic communication systems have been proposed to combat multipath fading [16, 17] over multipath fading channels. On the other hand, multi-antenna techniques are also applied for improving the performance and increasing the data rate of communication systems in WPAN, for example, single-input multiple-output (SIMO) architecture [18] based on chaotic modulation.

In this paper, we apply the cooperation technique to the FM-DCSK UWB system so as to construct a cooperative FM-DCSK UWB system. The bit-error-rate (BER) expressions of the proposed system with the error free (EF) protocol and decode-and-forward (DF) protocol are derived under indoor environments of IEEE 802.15.4a exploiting the moment generating function (MGF). Monte Carlo simulations performed over the IEEE 802.15.4a indoor channels not only validate the accuracy of the theoretical

BER formulas, but also show that the proposed system are remarkable superior to the conventional FM-DCSK UWB system through the cooperative diversity gain without increasing the implementation complexity. Furthermore, several critical parameters of the proposed system including integration interval and received antenna number at the destination are optimised such that the performance has been improved.

2 System model

In this section, we firstly introduce the multi-access FM-DCSK UWB system, and then present the system model of the cooperative FM-DCSK UWB scheme.

2.1 Multi-access FM-DCSK UWB system

Consider a FM-DCSK UWB system with U users. M ($M = 2U$)-order Walsh code is used to accommodate the U users. For example, given a two-user system, fourth-order Walsh code is adopted for realisation, which is constructed as follows

$$W_4 = \begin{bmatrix} w_1 \\ w_2 \\ w_3 \\ w_4 \end{bmatrix} = \begin{bmatrix} +1 & +1 & +1 & +1 \\ +1 & -1 & +1 & -1 \\ +1 & +1 & -1 & -1 \\ +1 & -1 & -1 & +1 \end{bmatrix} \quad (1)$$

Each user can select a couple of vectors to form the transmit signal. Assume that T_c is the pulse duration and $c(t)$ is the frequency-modulated chaotic carrier, we have $\int_0^{T_c} c^2(t)\,dt = 1$. Thus, the transmitted signal of the uth user can be expressed by

$$X(t) = \sum_{i=0}^{M-1} w_{2u-b^{(u)},i} \cdot c\left(t - i\frac{T}{M}\right), \qquad 0 < t < T \quad (2)$$

where $w_{m,n}$ denotes the element of m row n column of the M-order Walsh code and $b^{(u)}$ represents the transmitted bit of the uth user. The block diagram of the transmitter of the multi-access FM-DCSK UWB system is described in Fig. 1, where T is the bit duration.

During the demodulation process, the differential correlation (DC) demodulation should be replaced by the generalised maximum likelihood (GML) demodulation [19]. The block diagram of the GML demodulator of the kth received antenna for the uth user is plotted in Fig. 2, where T_d is the integration time.

Thus, the weighted energy of all the received antennas is accumulated to make a final decision. The total weighted energy for decision can be shown as

$$E_{GML} = \sum_{k=1}^{n} \int_{T-T_d}^{T} \left[\sum_{i=0}^{M-1} Y_k\left(t - i\frac{T}{M}\right) \cdot w_{2u-1,M-i} \right]^2 dt - \sum_{k=1}^{n} \int_{T-T_d}^{T} \left[\sum_{i=0}^{M-1} Y_k\left(t - i\frac{T}{M}\right) \cdot w_{2u,M-i} \right]^2 dt \quad (3)$$

where $Y_k\,(t - i(T/M))$ is the received signal of kth antenna that has a delay of iT/M. The decision will be '1' if $E_{GML} > 0$, otherwise '0'.

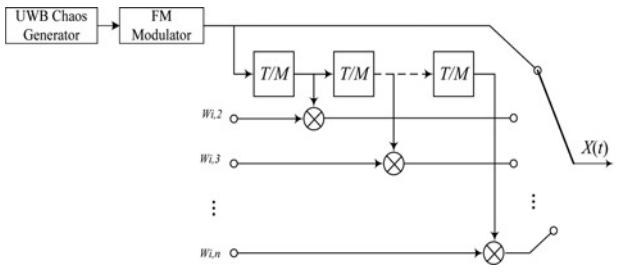

Fig. 1 *Block diagram of the transmitter in the FM-DCSK UWB system*

2.2 Cooperative FM-DCSK UWB system

The two-user cooperative FM-DCSK UWB system model with DF protocol is illustrated in Fig. 3. In the proposed cooperative system, the transmission period is divided into two time slots. In the first time slot, the source (user A) broadcasts its information through FM-DCSK modulation to both the relay and the destination. In the second time slot, if the relay (user B) can decode received signal correctly (for EF protocol, all the signals can be decoded successfully); it forwards the decoded information to the destination. Otherwise, the relay remains idle state. User B works in a similar way. In the rest sections, we assume that perfect synchronisation and perfect channel state information are available and the channel coefficients are independent for different transmit-receive links. Moreover, the equal-gain combiner (EGC) is adopted at the destination.

The received signals at the relay and each destination antenna can be expressed as

First time slot

$$\begin{aligned} Y_A^1(t) &= H_{B,A}(t) \otimes X_B(t) + N(t) \\ Y_B^1(t) &= H_{A,B}(t) \otimes X_A(t) + N(t) \\ Y_D^1(t) &= H_{A,D}(t) \otimes X_A(t) + H_{B,D}(t) \otimes X_B(t) + N(t) \end{aligned} \quad (4)$$

Second time slot

$$Y_D^2(t) = H_{A,D}(t) \otimes \tilde{X}_B(t) + H_{B,D}(t) \otimes \tilde{X}_A(t) + N(t) \quad (5)$$

where $\otimes$ is the convolution operator, $Y_A^1(t)$, $Y_B^1(t)$ and $Y_D^i(t)$ ($i = 1, 2$) denote the received signals at user A, user B and the destination, respectively. The superscript '1' and '2' represent the first time slot and second time slot, respectively. Moreover, $X_A(t)$ and $X_B(t)$ represent the transmitted signals of users A and B in the first time slot, respectively, whereas $\tilde{X}_A(t)$ and $\tilde{X}_B(t)$ denote the messages reconstructed by the relay corresponding to $X_A(t)$ and $X_B(t)$, respectively. $N(t)$ is a white Gaussian noise random variable with zero mean and two-sided power spectral density $N_0/2$. $H_{i,j}(t)$ ($i, j =$ A, B, D) is the channel impulse response of the indoor channel models, that is, CM1–CM4. As shown in the IEEE 802.15.4a standard, the channel impulse response is based on the Saleh–Valenzuela (SV) model [20]

$$H(t) = \sum_{i=1}^{N} \sum_{j=1}^{K} \alpha_{i,j} \delta(t - T_i - t_{i,j}) \quad (6)$$

where $\alpha_{i,j}$ is tap gain of the jth multipath component in the ith

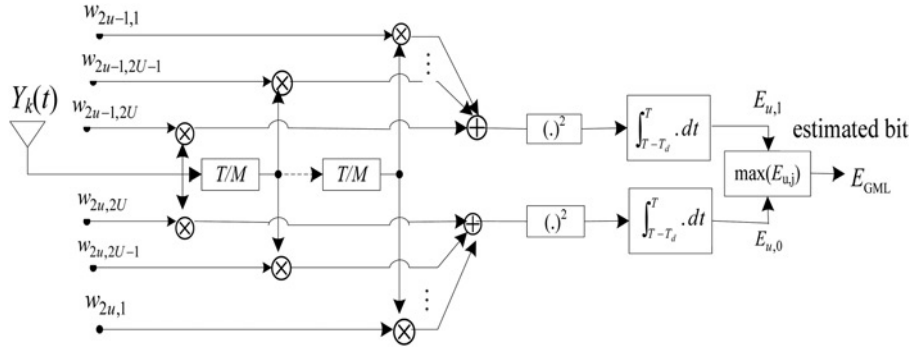

Fig. 2 *Block diagram of the GML detection in the FM-DCSK UWB system*

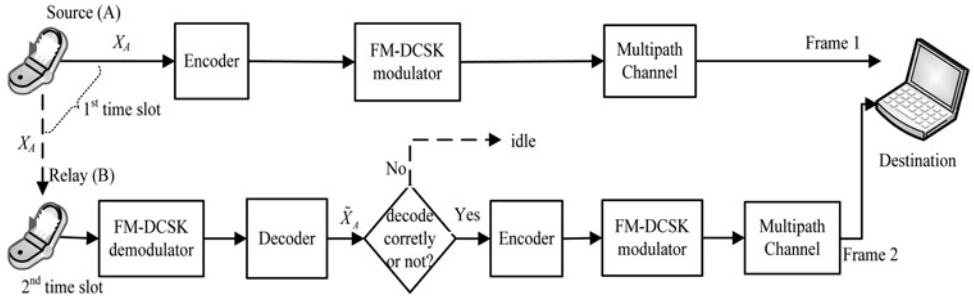

Fig. 3 *Block diagram of the cooperative FM-DCSK UWB system with DF protocol*

cluster, T_i is the delay of the ith cluster and $t_{i,j}$ is the delay of the jth path component relative to the ith cluster arrival time T_i.

To simplify the analysis, we can rewrite the channel response $H(t)$ as

$$H(t) = \sum_{l=1}^{L} \alpha_l \delta(t - \tau_l) \tag{7}$$

where L is the total number of the multipath component, α_l and τ_l denote the generalised gain and delay of the lth path component, respectively.

Considering the small-scale fading of IEEE 802.15.4a standard [20], in which the path gain is modelled as Nakagami distribution, that is, the probability density function (PDF) is given by

$$f_{|\alpha_l|}(\alpha) = \frac{2}{\Gamma(m_1)} \left(\frac{m_1}{\Omega_l}\right)^{m_1} \alpha^{2m_1-1} \exp\left(-\frac{m_1}{\Omega_l}\alpha^2\right) \tag{8}$$

where m_1 is the fading factor, Ω_l equals $E(\alpha_l^2)$ and $\Gamma(\cdot)$ denotes the gamma function. In this paper, we assume that each channel has a uniform scale parameter, meaning that Ω_i/m_i is kept constant for all the paths and the receiver knows all multipath parameters, that is, $\sum_{i=1}^{L} \Omega_i = \sum_{i=1}^{L} E(\alpha_i^2) = 1$.

Note that the cooperative SIMO FM-DCSK UWB system can be constructed if the number of received antennas at the destination is larger than one.

2.2.1 Comment about the integration interval: Fig. 4 shows the received signal structure of the cooperative FM-DCSK UWB system, where T is the bit duration, T_c is the duration of the chips and T_g is the guard interval duration between the reference and the information chips. In the conventional multi-access FM-DCSK UWB systems, the

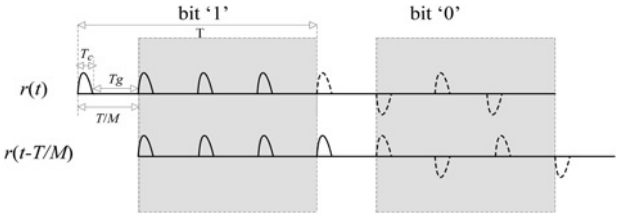

Fig. 4 *Received signal structure of the cooperative FM-DCSK UWB system*

integration interval T_d is set to T/M ($M = 4$). Nevertheless, Min *et al.* [10] illustrates that T_d should be carefully selected in $[T_c, T/M]$ to capture the most signal energy as well as the least noise energy and inter-pulse interference (IPI). Based on the above-mentioned analysis, the influence of T_d on the proposed system should be investigated and this parameter can be optimised by the 'binary search algorithm'. Binary search algorithm means that one can initialise the Monte Carlo simulation with $T_d = T/M$, and then perform other simulations as T_d decreases by half unless it is below T_c. Accordingly, we can find the best value of T_d through the comparison of the simulated results. The optimised result will be shown in Section 4.

3 Performance analysis

In this section, the performance of the two-user cooperative FM-DCSK UWB system is evaluated under IEEE 802.15.4a indoor environments. Before deriving the BER, we need to define some symbols. In a cooperative FM-DCSK UWB system, d_{SD}, d_{SR} and d_{RD} are used to denote the distance of source–destination (S–D) link, source–relay (S–R) link and relay–destination (R–D) link, respectively. Moreover, f_s denotes the sampling frequency. For ease of the analysis, we assume that d_{SD}:d_{SR}:d_{RD} = 1:1:1 and the

doi: 10.1049/iet-net.2011.0017

time delay of each path is much shorter than the pulse interval $\tau_l \ll T_c$.

The received signal-to-noise ratio (SNR) per bit γ_b at the receiver is defined as

$$\gamma_b = \frac{E_b}{N_0}\sum_{l=1}^{L}\gamma_l = \frac{E_b}{N_0}\sum_{l=1}^{L}\alpha_l^2 \tag{9}$$

where E_b is the bit energy, N_0 is the Gaussian noise power spectral density and γ_l is the instantaneous SNR of the lth path. It is well known that the square of a Nakagami random variable follows a gamma distribution. Moreover, the PDF of a gamma-distributed variable X with parameters $a > 0$ and $b > 0$, denoted as $X \sim G(a, b)$, is given by

$$f(x) = \frac{x^{a-1}e^{-x/b}}{b^a\,\Gamma(a)}, \quad x > 0 \tag{10}$$

Since α_l follows an m_l-Nakagami distribution, we have

$$\gamma_l = (E_b/N_0)\alpha_l^2 \sim G(m_l, (E_b/N_0)\,\Omega_l/m_l) \tag{11}$$

Combining (9) and (11) gives the distribution of the received SNR

$$\gamma_b \sim G\left(\sum_{l=1}^{L} m_l, \frac{E_b\sum_{l=1}^{L}\Omega_l}{N_0\sum_{l=1}^{l} m_l}\right) = G\left(mL, \frac{E_b/N_0}{\mathrm{mL}}\right) = G(x, y) \tag{12}$$

where $m_1 = m_2 = mL = m$, x and y are used as short-hand notations for mL and $(E_b/N_0)/(mL)$, respectively. Hence, the PDF of γ_b can be written as

$$f(\gamma_b) = \frac{\gamma_b^{x-1}e^{-\gamma_b/y}}{y^x\,\Gamma(x)} \tag{13}$$

In terms of the conclusion in [21], the conditional BER of the conventional non-cooperative FM-DCSK UWB system is expressed by

$$P(e|\gamma_b) = Q\left(\sqrt{\frac{E^2(b\prime)}{\mathrm{var}(b\prime)}}\right) = Q\left(\sqrt{\frac{\gamma_b^2}{2(\gamma_b + BT_c)}}\right) = Q\left(\sqrt{w}\right) \tag{14}$$

where $Q(\sqrt{w}) = (1/\pi)\int_0^{\pi/2} e^{-w/(2\sin^2\theta)}\,d\theta$, b' is the decoded bit, B is the equivalent bandwidth of the system or the bandwidth of Gaussian noise $N(t)$, $w = \gamma_b^2/2(\gamma_b + \mathrm{BT_c})$ denotes the received SNR of the decoded bit.

Hence, the average BER of the conventional FM-DCSK UWB system can be shown as

$$P_e(\gamma_b) = \int_0^{\infty} P(e|\gamma_b)f(\gamma_b)\,d\gamma_b \tag{15}$$

where $f(\gamma_b)$ is the PDF of γ_b.

Now we consider a dual-hop cooperative FM-DCSK UWB system with DF protocol including one source, one relay and one destination. The received SNR of the relay and the destination can be written as

$$\gamma_{SR} = \frac{E_{b,SR}}{N_0}\sum_{l=1}^{L}\alpha_{SR,l}^2 \tag{16}$$

$$\gamma_D = \frac{E_{b,SD}\sum_{l=1}^{L}\alpha_{SD,l}^2 + \tilde{E}_{b,RD}\sum_{l=1}^{L}\alpha_{RD,l}^2}{N_0} \tag{17}$$

where $E_{b,SR}$, $E_{b,SD}$ and $\tilde{E}_{b,RD}$ are the transmitted energy per bit of the S–R link, S–D link and R–D link, respectively. Moreover, $\alpha_{SR,l}$, $\alpha_{SD,l}$ and $\alpha_{RD,l}$ are the m-Nakagami-distributed fading parameters of the S–R link, S–D link and R–D link, respectively. We assume that $E_{b,SR} = E_{b,SD} = E_b$, and $\tilde{E}_{b,RD} = E_b$ if the relay decodes the signal successfully, otherwise $\tilde{E}_{b,RD} = 0$. In the following analysis, we denote that $\gamma_D = \gamma_{D1}$ if $\tilde{E}_{b,RD} = E_b$, while $\gamma_D = \gamma_{D2}$ if $\tilde{E}_{b,RD} = 0$.

Based on (12), we further derive the distribution of γ_{SR}, resulting in

$$\gamma_{SR} \sim G(mL, (E_b/N_0)/(mL)) = G(x, y) \tag{18}$$

As seen from (18), the PDF of γ_{SR} is the same as (13). Likewise, we obtain $\gamma_{D1} \sim G(2x, y)$ and $\gamma_{D2} \sim G(x, y)$.

The BER of the proposed system with DF protocol can be described as

$$P_e|_{DF} = (1 - P_e(\gamma_{SR}))P_e(\gamma_{D1}) + P_e(\gamma_{SR})P_e(\gamma_{D2}) \tag{19}$$

where $P_e(\gamma_{SR})$, $P_e(\gamma_{D1})$ and $P_e(\gamma_{D2})$ represent the BER at the relay, BER at the destination for $\tilde{E}_{b,RD} = E_b$ and the BER at the destination for $\tilde{E}_{b,RD} = 0$, respectively.

Substituting (13) [PDF of γ_{SR}, denoted as $f(\gamma_{SR})$] and (14) into (15), we have

$$\begin{aligned} P_e(\gamma_{SR}) &= \int_0^{\infty} P(e|\gamma_{SR})f(\gamma_{SR})\,d\gamma_{SR} \\ &= \int_0^{\infty} Q\left(\sqrt{w_{SR}}\right)f(w_{SR})\,dw_{SR} \\ &= \frac{1}{\pi}\int_0^{\pi/2}\int_0^{\infty} f(w_{SR})e^{-w_{SR}/2\sin^2\theta}\,d\,w_{SR}\,d\theta \end{aligned} \tag{20}$$

where $w_{SR} = \gamma_{SR}^2/[2(\gamma_{SR} + BT_c)]$. The MGF of a random variable w is defined as [22] $M_w(s) = \int_0^{\infty} e^{sw} f_\omega(w)\,dw$, applying this expression into (20) yields

$$P_e(\gamma_{SR}) = \frac{1}{\pi}\int_0^{\pi/2} M_{w_{SR}}(\mu_\theta)\,d\theta \tag{21}$$

where $\mu_\theta = -1/2\sin^2\theta$.

As shown in [21], the random variable w_{SR} also approximately follows a gamma distribution if γ_{SR} is a gamma-distributed variable, namely $\gamma_{SR} \sim G(x, y)$, denoted as $G(x_{SR}, x_{SR})$, where

$$\begin{cases} x_{SR} = x\left(\dfrac{\overline{\gamma}_{SR} + BT_c}{\overline{\gamma}_{SR} + 2BT_c}\right)^2 \\ y_{SR} = \dfrac{y\overline{\gamma}_{SR}(\overline{\gamma}_{SR} + 2BT_c)^2}{2(\overline{\gamma}_{SR} + BT_c)^3} \end{cases} \tag{22}$$

Here, $\overline{\gamma}_{SR} = \sum_{l=1}^{L}\overline{\gamma}_{SR,l} = (E_b/N_0)\sum_{l=1}^{L}E(\alpha_{SR,l}^2) = (E_b/N_0)$.

The MGF of a gamma-distributed random variable $w_{SR} \sim G(a_{SR}, b_{SR})$ can be written as [22]

$$M_{w_{SR}}(s) = (1 - sy_{SR})^{-x_{SR}} \tag{23}$$

Substituting (23) into (21) gives the following expression

$$P_e(\gamma_{SR}) \simeq \frac{1}{\pi}\int_0^{\pi/2} (1 - \mu_\theta y_{SR})^{-x_{SR}}\, d\theta \tag{24}$$

Similarly, the formulas of $P_e(\gamma_{D1})$ and $P_e(\gamma_{D2})$ [note that $P_e(\gamma_{D1})$ equals to the BER for the EF protocol] is given by

$$\begin{aligned} P_e|_{EF} = P_e(\gamma_{D1}) &= \frac{1}{\pi}\int_0^{\pi/2} M_{w_{D1}}(\mu_\theta)\, d\theta \\ &\simeq \frac{1}{\pi}\int_0^{\pi/2} (1 - \mu_\theta y_{D1})^{-x_{D1}} d\theta \end{aligned} \tag{25}$$

where $w_{D1} = \gamma_{D1}^2/[2(\gamma_{D1} + BT_c)]$ and

$$\begin{cases} x_{D1} = 2x\left(\dfrac{\overline{\gamma}_{D1} + BT_c}{\overline{\gamma}_{D1} + 2BT_c}\right)^2 \\ y_{D1} = \dfrac{y\overline{\gamma}_{D1}(\overline{\gamma}_{D1} + 2BT_c)^2}{2(\overline{\gamma}_{D1} + BT_c)^3} \end{cases} \tag{26}$$

and

$$\begin{aligned} P_e(\gamma_{D2}) &= \frac{1}{\pi}\int_0^{\pi/2} M_{w_{D2}}(\mu_\theta)\, d\theta \\ &\simeq \frac{1}{\pi}\int_0^{\pi/2} (1 - \mu_\theta y_{D2})^{-x_{D2}}\, d\theta \end{aligned} \tag{27}$$

where $w_{D2} = \gamma_{D2}^2/[2(\gamma_{D2} + BT_c)]$ and

$$\begin{cases} x_{D2} = x\left(\dfrac{\overline{\gamma}_{D2} + BT_c}{\overline{\gamma}_{D2} + 2BT_c}\right)^2 \\ y_{D2} = \dfrac{y\overline{\gamma}_{D2}(\overline{\gamma}_{D2} + 2BT_c)^2}{2(\overline{\gamma}_{D2} + BT_c)^3} \end{cases} \tag{28}$$

Putting (24), (25) and (27) into (19), we thus obtain the total BER of the proposed cooperative FM-DCSK UWB system as

$$\begin{aligned} P_e \simeq \frac{1}{\pi}\left(1 - \frac{1}{\pi}\int_0^{\pi/2} (1 - \mu_\theta y_{SR})^{-x_{SR}}\, d\theta\right)\int_0^{\pi/2} (1 - \mu_\theta y_{D1})^{-x_{D1}}\, d\theta \\ + \frac{1}{\pi^2}\int_0^{\pi/2} (1 - \mu_\theta y_{SR})^{-x_{SR}}\, d\theta \int_0^{\pi/2} (1 - \mu_\theta y_{D2})^{-x_{D2}}\, d\theta \end{aligned} \tag{29}$$

Consequently, given the specific channel model parameters of IEEE 802.15.4a indoor environments, that is, CM1–CM4, we can calculate the theoretical BER of the proposed cooperative FM-DCSK UWB system.

4 Simulation results and discussions

In this section, the numerical and Monte Carlo simulated results of the proposed two-user cooperative FM-DCSK UWB system are performed under indoor channels of the IEEE 802.15.4a, based on line-of-sight (LOS) indoor residential (CM1), NLOS indoor residential (CM2), LOS indoor office (CM3) and NLOS indoor office environments (CM4), respectively. Furthermore, we optimise the integration interval by adopting the binary search algorithm and discuss the effect of the number of receive antennas at the destination on the BER performance of the proposed system. Unless otherwise mentioned, we assume that the cubic chaotic map is chosen for chaotic pulse generation, the DF relaying protocol is adopted and the channel impulse response is invariant in a frame, that is, E_b is kept constant. Also, the number of received antennas is set to 1 (i.e. $n = 1$). Other simulation parameters are shown in Table 1.

4.1 Performance comparison between the conventional multi-access FM-DCSK UWB system and the proposed cooperative FM-DCSK UWB system

Here, we show the merit of the proposed cooperative FM-DCSK UWB systems with DF protocol. For comparison, the conventional non-cooperative FM-DCSK UWB and the cooperative FM-DCSK UWB system with EF protocol are used to gauge the performance. The results are presented in Fig. 5, in which the CM1 channel environment is assumed. The parameters used are following those for CM1 [20]. Referring to this figure, the BER performance proposed cooperative FM-DCSK UWB system with DF is almost the same as that of EF and both of the two cases have performance gains about 2 dB over the conventional one at a BER of 2×10^{-4} in CM1 owing to the cooperative diversity gain. Moreover, we observe that all the simulated BER curves are highly consistent with the theoretical results in Section 3. Simulations have also been performed in other channel models and similar observations are obtained.

4.2 Performance comparison of the proposed cooperative FM-DCSK UWB system among different channel models

Fig. 6 plots the simulated BER curves of the proposed cooperative FM-DCSK UWB system in CM1–CM4. As seen from this figure, the performance of proposed system in CM4 is superior to that in other three-channel models, showing the best BER performance, while the system performs worst in CM2. For example, at $E_b/N_0 = 17$ dB, the proposed system in CM2 and CM1 merely achieve BERs of 5×10^{-5} and 3×10^{-5}, respectively, while it can accomplish BERs of 2×10^{-5} and 1×10^{-5} in CM3 and CM4, respectively. In general, the channel models in which the proposed system performs best to worst are in the following order: (i) CM4, (ii) CM3, (iii) CM1 and (iv) CM2.

Table 1 Simulation parameters

Parameter	Value
pulse duration (T_c)	2.5 ns
bit duration (T)/bit rate (v)	400 ns (2.5 Mbits/s)
integration interval (T_d)	50 ns
sampling frequency (f_s)	8 GHz
d_{SD}:d_{SR}:d_{RD}	1:1:1

doi: 10.1049/iet-net.2011.0017

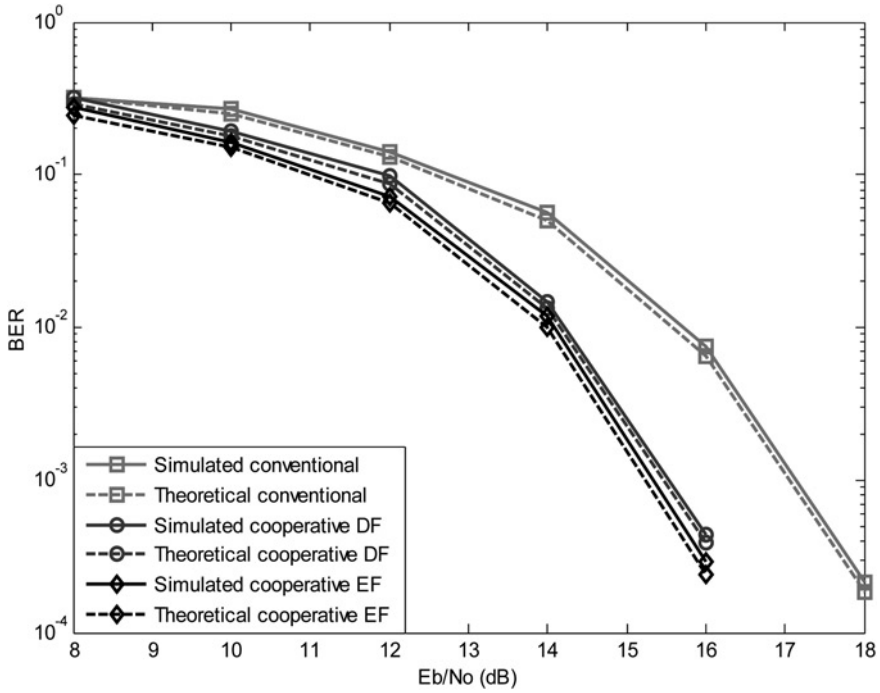

Fig. 5 *BER performance of the conventional multi-access FM-DCSK UWB system and proposed cooperative FM-DCSK UWB system in CM1*

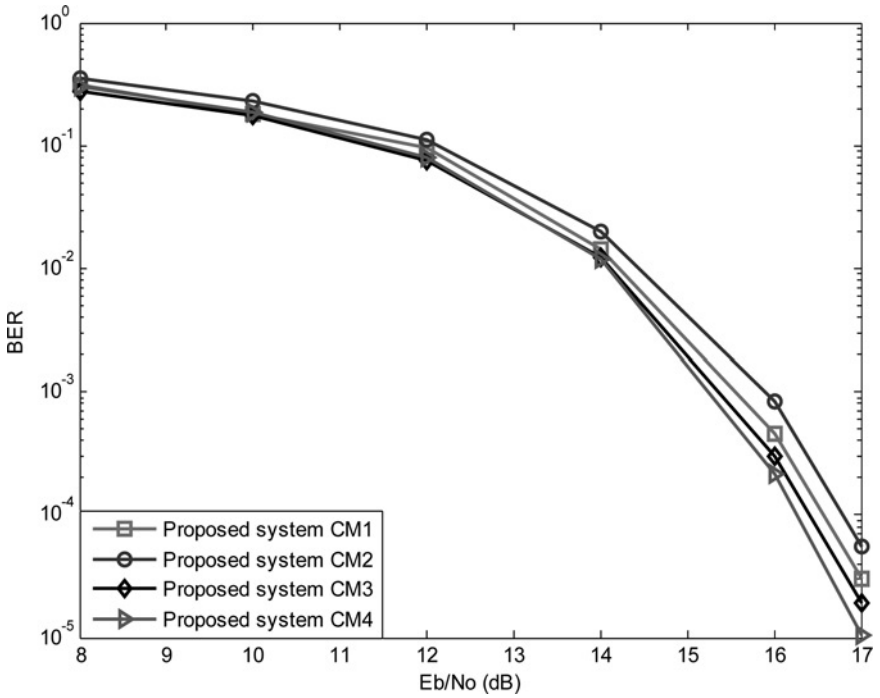

Fig. 6 *BER performance of the proposed cooperative FM-DCSK UWB system in different channel models, that is, CM1, CM2, CM3 and CM4*

4.3 Discussion about the number of received antennas (cooperative SIMO FM-DCSK UWB system) and the integration interval

Firstly, we adopt multiple ($n > 1$) received antennas to investigate the performance of the cooperative SIMO FM-DCSK UWB system, while other parameters used are the same as Section 4.1. Fig. 7 shows the BER performance of the system with different received antenna numbers in CM1. It indicates that the system performance is improved as antenna number n increases by means of obtaining the spatial diversity gain. However, the multiple-antenna scheme has some drawbacks: (i) the performance gain is decreasing gradually as n becomes larger since the transmitted energy per bit (i.e. total energy of all the transmit-receive antenna pairs) is constant and (ii) the system complexity is growing at the same time. We also observe that the performance gain can almost be neglected when n is larger than five. Accordingly, $n = 5$ is considered as the optimised value to realise the goal of achieving a trade-off between performance and system complexity.

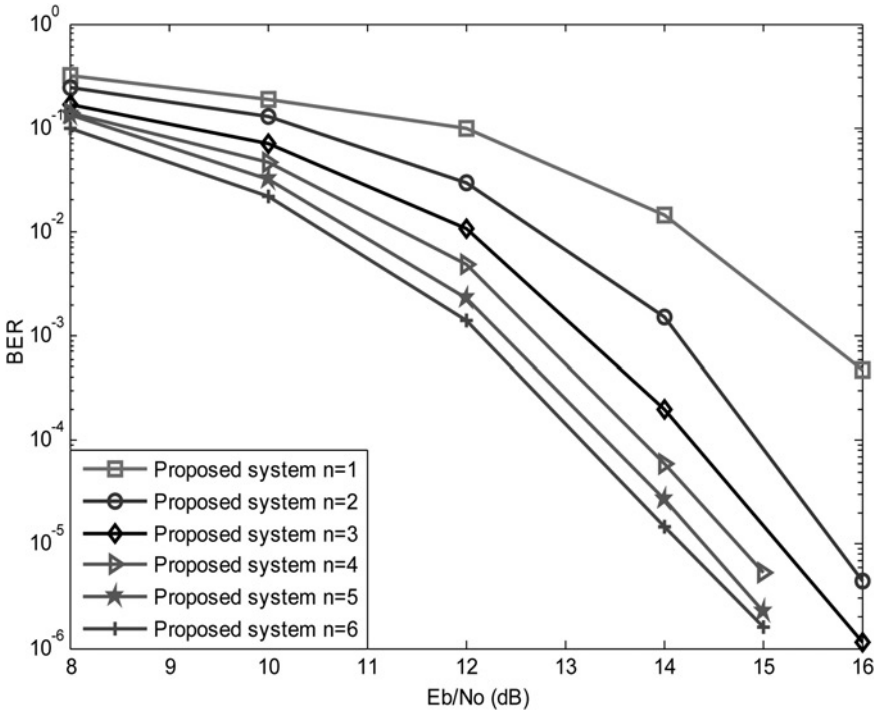

Fig. 7 *BER performance of the proposed system with different received antenna numbers in CM1*

As described in Section 2, integration interval T_d is a significant parameter for the system performance. Thus, it is necessary to study the effect of T_d ($T_d \in [T_s, T/M]$, that is, [2.5, 100 ns]) on the proposed cooperative SIMO FM-DCSK UWB system. For simple analysis, we adopt the binary search algorithm to optimise this parameter. In other words, we perform the simulations begin with $T_d = 100$ ns, then we gradually decrease the integration interval by half (i.e. $T_d' = T_d/2$) for other simulations unless it is below 2.5 ns (T_s). The BER performance of the proposed system with different integration interval values T_d in CM1 is shown in Fig. 8. The parameters used are the same as Section 4.1 except that T_d now varies and n is set to 2. Referring to this figure, the BER performance is significant improved as T_d decreases from 100 ns to 25 ns. Yet, once T_d is smaller than 25 ns, it is found that the BER performance will be deteriorated with the further decreasing of T_d. This phenomenon may attribute to much severer IPI when the T_d is less than a certain value, although less noise energy exits for a small T_d. As a result, we should carefully choose T_d in order to capture the most signal energy as well as the least noise energy and IPI. In our case, $T_d = 25$ ns is the best value.

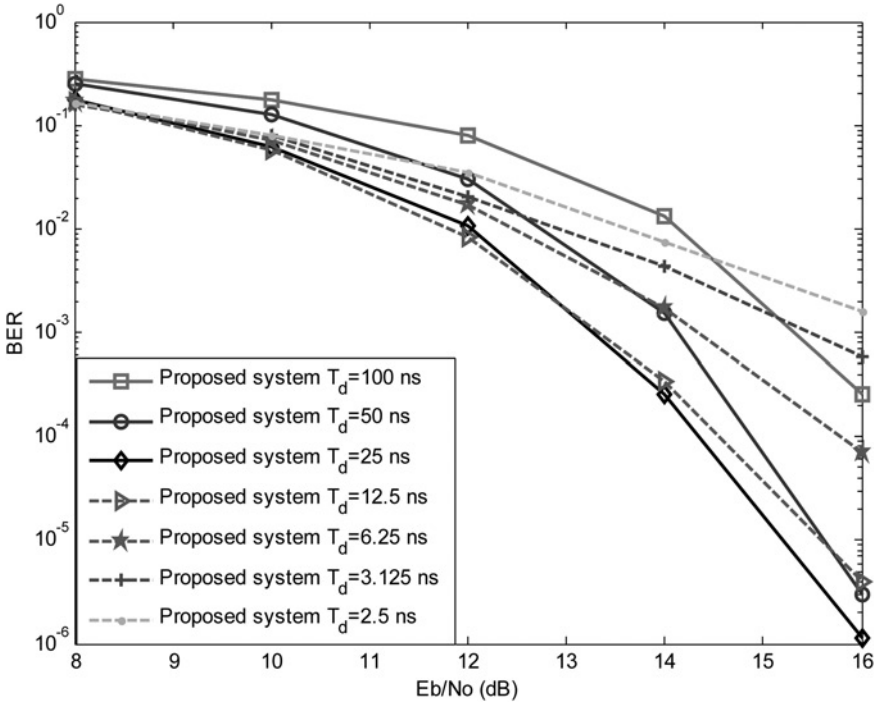

Fig. 8 *BER performance of the proposed system with different integration interval values in CM1*

doi: 10.1049/iet-net.2011.0017

5 Conclusions

In this paper, the cooperative architecture was adopted for the FM-DCSK UWB system to achieve the spatial diversity gain without increasing the implementation complexity. The BER performance analysis of the proposed system is provided for such a system. Monte Carlo simulations showed that the proposed system has a gain about 2 dB compared to the conventional one at a BER of 2×10^{-4} under indoor environments of IEEE 802.15.4a, which agrees well with the theoretical results. Furthermore, several critical parameters, for example, the received antenna number of destination and integration interval, were optimised and thus found that $n = 5$ and $T_d = 25$ ns were the optimal values to achieve the best BER performance through simulated results. The proposed cooperative FM-DCSK UWB system can be easily extended to more than two users by modifying the cooperative protocol. Based on the superiorities of excellent BER performance and relatively low complexity, the cooperative FM-DCSK UWB system is believed to be a competitive scheme for the low-rate and low-power WPAN and WSN applications.

6 Acknowledgment

The authors would like to thank Jing Xu for her valuable discussion and to thank the anonymous reviewers for their constructive comments that have helped improving the overall quality of the paper. This research was partially supported by the NSF of China (Nos. 60972053, 61001073 and 61102134), the European Union-FP7 (CoNHealth, No. 294923), as well as the Fundamental Research Funds for the Central Universities (No. 201112G017).

7 References

1 Gerrits, J., Farserotu, J., Long, J.: 'Low complexity ultra-wide-band communications', *IEEE Trans. Circuits Syst.-II*, 2008, **55**, (4), pp. 757–760
2 IEEE 802.15.4a Task Group: 'WPAN Low Rate Alternative PHY'. Available at http://www.ieee802.org/15/pub/TG4a.html
3 Chong, C., Yong, S., Kim, Y., *et al.*: 'Samsung Electronics (SAIT) CFP presentation for IEEE 802.15.4a alternative PHY', IEEE 802.15-05-0030-02-004a, 2005
4 Lee, H., Lee, C., Park, D., *et al.*: 'Chaotic pulse based communication system proposal', IEEE 802.15-05-0010-04-004a, 2005
5 Kolumbán, G., Kennedy, M., Kis, G., Jákó, Z.: 'FM-DCSK: a novel method for chaotic communications'. Proc. IEEE Int. Symp. on Circuits and Systems, May 1998, pp. 477–480
6 Kennedy, M., Kolumbán, G., Kis, G., Jákó, Z.: 'Performance evaluation of FM-DCSK modulation in multipath environments', *IEEE Trans. Circuits Syst.-I.*, 2000, **47**, (12), pp. 1702–1711
7 Ye, L., Chen, G., Wang, L.: 'Essence and advantages of FM-DCSK versus conventional spread-spectrum communication methods', *Circuits, Syst. Signal Process.*, 2005, **24**, (5), pp. 657–673
8 Kolumbán, G.: 'UWB technology: chaotic communications versus noncoherent impulse radio'. Proc. European Conf. on Circuit Theory and Design., August 2005, vol. 2, pp. 79–82
9 Chong, C., Yong, S.: 'UWB direct chaotic communication technology for low-rate WPAN applications', *IEEE Trans. Veh. Technol.*, 2008, **57**, (3), pp. 1527–1536
10 Min, X., Xu, W., Wang, L., Chen, G.: 'Promising performance of an FM-DCSK UWB system under indoor environments', *IET Commun.*, 2010, **4**, (2), pp. 125–134
11 Chen, S., Wang, L., Chen, G.: 'Data-aided timing synchronization for FM-DCSK UWB communication system', *IEEE Trans. Ind. Electron.*, 2010, **57**, (5), pp. 1538–1545
12 Chao, H., Chang, C., Chen, C., Chang, K.: 'Survey of cross-layer optimization techniques for wireless networks'. Chapter 21 of the fourth-generation wireless networks: applications and innovations, IGI Global, 2009
13 Sendonaris, A., Erkip, E., Aazhang, B.: 'User cooperation diversity – Part I: system description', *IEEE Trans. Commun.*, 2003, **51**, (11), pp. 1927–1938
14 Sendonaris, A., Erkip, E., Aazhang, B.: 'User cooperation diversity – Part II: implementation aspects and performance analysis', *IEEE Trans. Commun.*, 2003, **51**, (11), pp. 1939–1948
15 Chen, C., Chang, K., Chao, H., Chen, J.: 'Extending emergency services coverage in cooperative IMS networks', *J. Auton. Adapt. Commun. Syst. (IJAACS)*, 2012, **5**, (4), pp. 417–434
16 Xu, J., Xu, W., Wang, L., Chen, G.: 'Design and simulation of a cooperation communication system based on DCSK/FM-DCSK'. Proc. IEEE Int. Symp. on Circuits and Systems, May 2010, vol. 4, pp. 2454–2457
17 Xu, W., Wang, L., Chen, C.: 'Performance of DCSK cooperative communication systems over multipath fading channels', *IEEE Trans. Circuits Syst.-I*, 2011, **50**, (1), pp. 196–204
18 Wang, L., Zhang, C., Chen, G.: 'Performance of an SIMO FM-DCSK communication system', *IEEE Trans. Circuits Syst.-II*, 2008, **55**, (5), pp. 457–461
19 Kolumbán, G., Kis, G., Lau, F., Tse, C.: 'Optimum noncoherent FM-DCSK detector: application of chaotic GML decision rule'. Proc. IEEE Int. Symp. on Circuits and Systems, May 2004, vol. 4, pp. IV-597–600
20 Molisch, A., Balakrishnan, K., Cassioli, D., *et al.*: 'IEEE 802.15.4a channel model-final report' IEEE 802.15-04-0662-00-004a, 2005
21 Pausini, M., Janssen, G.: 'Performance analysis of UWB autocorrelation receivers over Nakagami-fading channels', *IEEE J. Sel. Topoics in Signal Process.*, 2007, **1**, (3), pp. 433–445
22 Simon, M., Alouini, M.: 'Digital communication over fading channels' (Wiley, Chichester, UK, 2005, 2nd edn.)